

# X-ray, IR and bulk magnetic properties of $\text{Cu}_{1+x}\text{Mn}_x\text{Fe}_{2-2x}\text{O}_4$ ferrite system

D. S. BIRAJDAR, U. N. DEVATWAL, K. M. JADHAV  
 Department of Physics, Dr. Babasaheb Ambedkar Marathwada University,  
 Aurangabad 431004, India

The structural, IR and magnetic properties of the mixed spinel  $\text{Cu}_{1+x}\text{Mn}_x\text{Fe}_{2-2x}\text{O}_4$  ( $x = 0.0, 0.1, 0.2, 0.3, 0.4, 0.5$  and  $0.6$ ) system have been investigated by means of X-ray diffraction, Infrared spectroscopy, magnetization and a.c. susceptibility measurements. X-ray results confirm single-phase spinel structure for all the concentrations. The structure of  $\text{CuFe}_2\text{O}_4$  is tetragonal and changes to cubic for  $x = 0.1$  to  $0.4$ . For  $x = 0.5$  and  $0.6$  the structure become tetragonal. The lattice parameter and X-ray density are deduced and their variation with  $\text{Mn}^{4+}$  concentration is studied. The cation distribution derived from the X-ray diffractometry data was found to agree very well with the cation distribution obtained from magnetization measurements. X-ray intensity calculations indicate that  $\text{Mn}^{4+}$  occupy only octahedral [B] sites and  $\text{Cu}^{2+}$  and  $\text{Fe}^{3+}$  ions occupy both octahedral [B] and tetrahedral (A) sites. The infrared spectra obtained at room temperature in the range  $200\text{--}800\text{ cm}^{-1}$  showed two absorption bands. The force constants have been obtained from IR data. The variation of the saturation magnetization per formula unit as a function of  $\text{Mn}^{4+}$  content  $x$  has been satisfactorily explained on the basis of Neel's collinear spin ordering model for all values of  $x$ . The Curie temperature  $T_C$  determined from a.c. susceptibility data decreases with increase of  $\text{Mn}^{4+}$  concentration  $x$ , suggesting decrease in ferrimagnetic behaviour.

© 2002 Kluwer Academic Publishers

## 1. Introduction

Ferrites have been the subject of extensive study because of their wide range of applications and of their importance in understanding the theories of magnetism. They exhibit interesting structural, electrical and magnetic properties which may depend upon the nature of ions and their charge, the preparation method and ability to distribute the cations amongst the available tetrahedral (A) and octahedral [B] sites [1]. This so called as cation distribution is proved to be an equilibrium function of temperature, pressure and composition [2, 3]. Extensive works have been carried out by various workers to upgrade the properties of ferrites by substituting different types and amounts of impurities.

Copper ferrite and copper containing ferrites have been a focus of continuous interest in the recent years. The ferromagnetic spinel copper ferrite shows remarkable variation of its structure and consequently of its magnetic properties depending on the heat treatment. Copper ferrite is highly sensitive to heat treatment [4], shows tetrahedral structure and semiconductive property [5]. When copper ferrite is quenched from higher temperature it shows switching and memory phenomenon [6]. The influence of Jahn-Teller ions  $\text{Cu}^{2+}$  at the octahedral [B] sites can be modified by trivalent and tetrahedral ions [7–9]. Many workers have reported the influence of tetrahedral ions like  $\text{Ti}^{4+}$ ,  $\text{Ge}^{4+}$ ,  $\text{Sn}^{4+}$ ,  $\text{Si}^{4+}$  and  $\text{Zr}^{4+}$  on the properties of copper ferrite [10–12].

The aim of the present work is to study the effect of  $\text{Mn}^{4+}$  on the structural, IR and magnetic properties of copper ferrite.

Here we report structural, IR and magnetic properties of solid solutions series  $\text{Cu}_{1+x}\text{Mn}_x\text{Fe}_{2-2x}\text{O}_4$  with  $x = 0.0, 0.1, 0.2, 0.3, 0.4, 0.5$  and  $0.6$  studies by means of X-ray diffraction, Infrared spectroscopy, magnetization and ac susceptibility measurements.

## 2. Experimental

The samples of the spinel solid solution series  $\text{Cu}_{1+x}\text{Mn}_x\text{Fe}_{2-2x}\text{O}_4$  with  $x = 0.0, 0.1, 0.2, 0.3, 0.4, 0.5$  and  $0.6$  were prepared by using conventional ceramic technique. The appropriate quantities of ferric oxide ( $\text{Fe}_2\text{O}_3$ ), manganese dioxide ( $\text{MnO}_2$ ) and copper oxide ( $\text{CuO}$ ) all 99.9% pure and supplied by E. Merck, were thoroughly mixed in stoichiometric proportions and were ground. These mixtures in powder form were pressed in to circular pellets and fired at  $750^\circ\text{C}$  for 12 h. in muffle furnace. The pellet were furnace cooled, ground in to fine powder, repelletized and refired at  $980^\circ\text{C}$  for 24 h. The pellets were slowly cooled at the rate of  $2^\circ\text{C}/\text{min}$ . The pellets were found to be crack-free, flat and hard. The X-ray powder diffractions were recorded using  $\text{Cu K}_\alpha$  radiation on philips X-ray diffractometer (Model 3710). The infrared spectra of ferrite samples were recorded by using Perkin Elmer infrared spectrophotometer in the range  $200\text{--}800\text{ cm}^{-1}$ .

For recording IR spectra, powders were mixed with KBr in the ratio 1 : 250 by weight to ensure uniform dispersion in the KBr pellet. The mixed powders were pressed in a cylindrical die to get clean discs of approximately 1 mm thickness. The high field magnetization (300 K) measurements were carried out using high field hysteresis loop technique [13]. The a.c. susceptibility of powdered samples was measured using the double coil set up [14].

### 3. Results and discussion

The room temperature X-ray diffraction patterns showed sharp lines corresponding to single-phase spinel structure for all the samples. Fig. 1 depicts X-ray diffractograms for  $x = 0.2, 0.4$  and  $0.6$  samples. The values of lattice parameter determined from X-ray data with an accuracy of  $\pm 0.002 \text{ \AA}$  for all the samples are summarized in Table I. It is observed from Table I that the ratio  $c/a > 1$  for  $x = 0.0, 0.5$  and  $0.6$  which indicates that structure is tetragonal. For  $x = 0.1$  to  $0.4$ , the ratio  $c/a = 1$ , suggesting crystal structure is cubic. This behaviour of lattice parameter is in agreement with  $\text{Ge}^{4+}$  substituted copper ferrites [15]. It is evident from Table I that lattice parameter  $a$  decreases (linearly) with increase in  $\text{Mn}^{4+}$  content  $x$  from  $x = 0.1$  to  $0.6$ . The

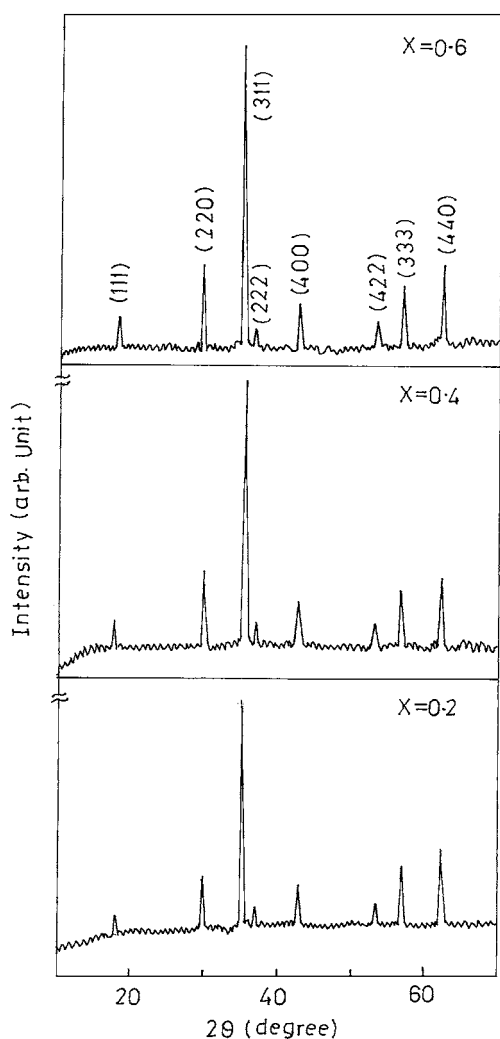


Figure 1 Typical X-ray diffractograms of  $\text{Cu}_{1+x}\text{Mn}_x\text{Fe}_{2-2x}\text{O}_4$  for  $x = 0.2, 0.4, 0.6$ .

TABLE I Lattice constant ( $a$  and  $c/a$ ), phase and X-ray density for  $\text{Cu}_{1+x}\text{Mn}_x\text{Fe}_{2-2x}\text{O}_4$

Composition ( $x$ )	$a$ ( $\text{\AA}$ )	$c/a$	Phase	X-ray density $d_x$ ( $\text{gm/cm}^3$ )
$\text{CuFe}_2\text{O}_4$	$a = 8.298$ $c = 9.572$	1.15	Tetragonal	4.819
$\text{Cu}_{1.1}\text{Mn}_{0.1}\text{Fe}_{1.8}\text{O}_4$	8.399	1.00	Cubic	5.376
$\text{Cu}_{1.2}\text{Mn}_{0.2}\text{Fe}_{1.6}\text{O}_4$	8.390	1.00	Cubic	5.408
$\text{Cu}_{1.3}\text{Mn}_{0.3}\text{Fe}_{1.4}\text{O}_4$	8.388	1.00	Cubic	5.428
$\text{Cu}_{1.4}\text{Mn}_{0.4}\text{Fe}_{1.2}\text{O}_4$	$a = 8.379$	1.00	Cubic	5.460
$\text{Cu}_{1.5}\text{Mn}_{0.5}\text{FeO}_4$	$a = 8.332$ $c = 10.563$	1.21	Tetragonal	4.693
$\text{Cu}_{1.6}\text{Mn}_{0.6}\text{Fe}_{0.8}\text{O}_4$	$a = 8.316$ $c = 10.147$	1.22	Tetragonal	4.603

variation of lattice parameter  $a$  with  $x$  can be explained on the basis of ionic radii of substituted ion [16]. The observed decrease in  $a$  with  $x$  is due to the replacement of larger ionic crystal radius of  $\text{Fe}^{3+}$  ( $0.64 \text{ \AA}$ ) by smaller  $\text{Mn}^{4+}$  ( $0.52 \text{ \AA}$ ).

The X-ray density for all the samples was calculated using the relation [17]

$$d_x = \frac{Z \cdot M}{N \cdot V} \quad (1)$$

where  $Z$  is the number of molecules per unit cell ( $z = 8$ ),  $M$  is the molecular weight,  $N$  is Avogadro's number, and  $V$  is the volume of the unit cell ( $V = a^2c$  for tetragonal and  $v = a^3$  for cubic). The values of X-ray density are listed in Table I. It is seen from Table I that the X-ray density increases with increase in  $\text{Mn}^{4+}$  content  $x$ . The increase in X-ray density ( $d_x$ ) is attributed to the decrease in lattice parameter  $a$  with  $x$ .

The cation distribution in spinel ferrites can be obtained from the analysis of X-ray diffraction [18], Mossbauer effect [19] and magnetization data [20]. In the present paper the cation distribution is estimated from magnetization (300 K) and X-ray intensity calculations.

In order to determine the cation distribution X-ray intensity calculations were carried out and compared with the observed ones. The absorption and temperature factors are not taken in to account in our calculations, because these do not affect the relative intensity calculations for spinels at a room temperature [21]. The ratio of intensities of reflections due to the planes (220) and (440) have been chosen as a criterion to determine the cation distribution. The XRD intensity calculations were carried out according to the formula suggested by Buerger [22]

$$I_{hkl} = |F_{hkl}|^2 P \cdot L_p \quad (2)$$

Where  $I_{hkl}$  is the relative integrated intensity,  $F_{hkl}$  is the structure factor,  $P$  the multiplicity factor for the plane ( $hkl$ ) and  $L_p$  the Lorentz polarization factor.

$$L_p = (1 + \cos^2 2\theta) / (\sin^2 \theta \cdot \cos \theta) \quad (3)$$

The formulae for the structure factors for the planes ( $hkl$ ) given by Furahashi *et al.* [23] have been used.

TABLE II Cation distribution for the  $\text{Cu}_{1+x}\text{Mn}_x\text{Fe}_{2-2x}\text{O}_4$

Composition (x)	Cation distribution		$\text{Fe}^{3+}$ tetra $\text{Fe}^{3+}$ octa
	A-site	B-site	
$\text{CuFe}_2\text{O}_4$	$\text{Fe}_{0.96}^{3+}\text{Cu}_{0.04}^{2+}$	$\text{Fe}_{1.04}^{3+}\text{Cu}_{0.96}^{2+}$	0.96
$\text{Cu}_{1.1}\text{Mn}_{0.1}\text{Fe}_{1.8}\text{O}_4$	$\text{Fe}_{0.9}^{3+}\text{Cu}_{0.1}^{2+}$	$\text{Fe}_{0.9}^{3+}\text{Mn}_{0.1}^{4+}\text{Cu}^{2+}$	1.00
$\text{Cu}_{1.2}\text{Mn}_{0.2}\text{Fe}_{1.6}\text{O}_4$	$\text{Fe}_{0.83}^{3+}\text{Cu}_{0.17}^{2+}$	$\text{Fe}_{0.77}^{3+}\text{Mn}_{0.2}^{4+}\text{Cu}_{1.03}^{2+}$	1.07
$\text{Cu}_{1.3}\text{Mn}_{0.3}\text{Fe}_{1.4}\text{O}_4$	$\text{Fe}_{0.78}^{3+}\text{Cu}_{0.22}^{2+}$	$\text{Fe}_{0.62}^{3+}\text{Mn}_{0.3}^{4+}\text{Cu}_{1.08}^{2+}$	1.25
$\text{Cu}_{1.4}\text{Mn}_{0.4}\text{Fe}_{1.2}\text{O}_4$	$\text{Fe}_{0.72}^{3+}\text{Cu}_{0.28}^{2+}$	$\text{Fe}_{0.48}^{3+}\text{Mn}_{0.4}^{4+}\text{Cu}_{0.15}^{2+}$	1.50

The formulae for the multiplicity factor and Lorentz polarization factors are taken from literature [17].

In the present system  $\text{Cu}_{1+x}\text{Mn}_x\text{Fe}_{2-2x}\text{O}_4$  of ferrites variation of  $\text{Mn}^{4+}$  concentration  $x$  results in the replacement of  $2x\text{Fe}^{3+}$  ions by  $x\text{Mn}^{4+}$  and  $x\text{Cu}^{2+}$  ions. In accordance with the site preference energies, the  $\text{Cu}^{2+}$ ,  $\text{Mn}^{4+}$  ions occupy B sites, whereas  $\text{Fe}^{3+}$  ion shows no definite site preference [24]. In determining the cation distribution of  $\text{Cu}_{1+x}\text{Mn}_x\text{Fe}_{2-2x}\text{O}_4$  system, we have assumed the cation distribution of  $\text{CuFe}_2\text{O}_4$  as [25]  $(\text{Cu}_{0.4}\text{Fe}_{0.6})^{\text{A}}(\text{Cu}_{0.6}\text{Fe}_{1.4})^{\text{B}}$ . The distribution of divalent, trivalent and tetravalent cations amongst tetrahedral (A) and octahedral [B] sites in the  $\text{Cu}_{1+x}\text{Mn}_x\text{Fe}_{2-2x}\text{O}_4$  was determined from the ratio of X-ray diffraction line  $I_{220}/I_{440}$  and  $I_{422}/I_{440}$ . The results of X-ray intensity calculations for various possible models have been tried and were compared with the observed intensity ratio for  $x = 0.1$  to  $0.4$  (i.e. cubic phase). The calculated intensity ratio, which agrees with the observed ratios, is depicted in Fig. 2. It is observed from Fig. 2 that, the calculated  $I_{220}/I_{440}$  and  $I_{422}/I_{440}$  ratios for  $x = 0.1$  to  $0.4$  are in good agreement with the experimentally determined  $I_{220}/I_{440}$  and  $I_{422}/I_{440}$  ratios. The cation distribution estimated from X-ray diffraction intensity ratio calculations are summarized in Table II for  $x = 0.0$  to  $0.4$ . It is evident from cation distribution (Table II and Fig. 2) that,  $\text{Mn}^{4+}$  ion occupies octahedral [B] sites whereas  $\text{Cu}^{2+}$  ions occupy both tetrahedral (A) and octahedral [B] sites. The amount of  $\text{Cu}^{2+}$  at tetrahedral (A) site goes on increasing as  $x$  increases from  $x = 0.1$  to  $0.4$ . The Jahn-Teller

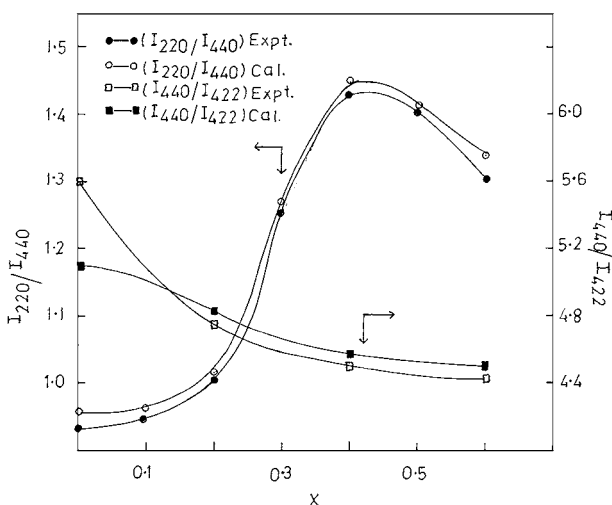


Figure 2 Variation of X-ray intensity ratios ( $I_{220}/I_{440}$ ) and ( $I_{440}/I_{422}$ ) with  $\text{Mn}^{4+}$  content  $x$  ( $x = 0.1$  to  $0.4$ ).

distortions of Cu ions in spinels have been discussed by Goodenough and Loeb [24]. According to their analysis Cu ions at tetrahedral A site give local distortion of the tetrahedral site with  $c/a > 1$  and Cu ions at the [B] site give an opposite distortion migration of B site to A site reduces tetragonality and structure becomes cubic. The occupancy of Cu ions at A and B sites was calculated from cation distribution (Table II). Fig. 3 shows the ratio of Cu ions at A site to total Cu ions in the system versus  $\text{Mn}^{4+}$  concentration for  $x = 0.0$  to  $0.4$ .

The IR spectra of the series  $\text{Cu}_{1+x}\text{Mn}_x\text{Fe}_{2-2x}\text{O}_4$  for  $x = 0.0, 0.2$  and  $0.4$  are shown in Fig. 4. The spectra

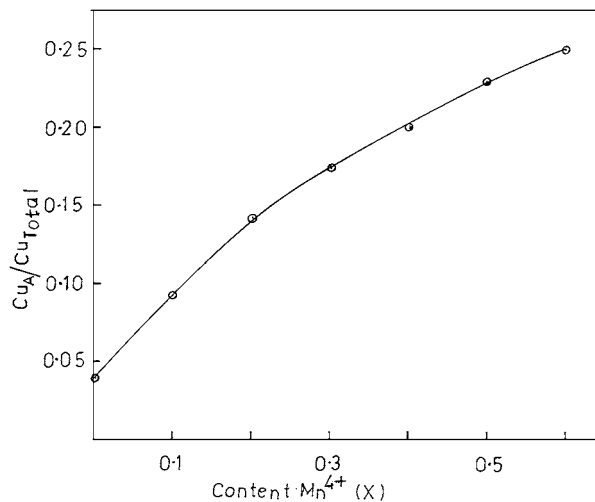


Figure 3 Variation of  $\text{Cu}_A/\text{Cu}_{\text{Total}}$  with  $\text{Mn}^{4+}$  content  $x$  ( $x = 0.0$  to  $0.4$ ).

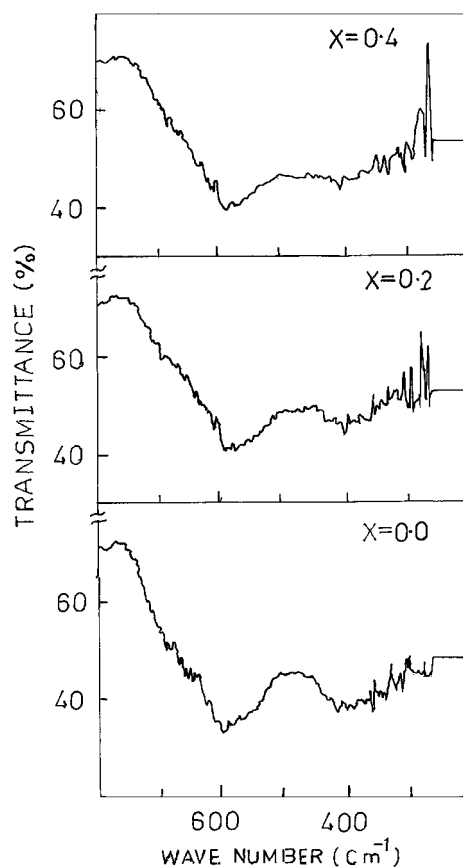


Figure 4 Infrared spectrograph of  $\text{Cu}_{1+x}\text{Mn}_x\text{Fe}_{2-2x}\text{O}_4$  for  $x = 0.0, 0.2, 0.4$ .

TABLE III Lattice vibration  $\nu_1$ ,  $\nu_2$ , force constants  $k_0$ ,  $k_t$ , and bond length  $R_A$ ,  $R_B$  for  $\text{Cu}_{1+x}\text{Mn}_x\text{Fe}_{2-2x}\text{O}_4$ 

Composition ( $x$ )	$\nu_1$ ( $\text{cm}^{-1}$ )	$\nu_2$ ( $\text{cm}^{-1}$ )	$K_0$ (dynes/cm)	$K_t$ (dynes/cm)	$R_A$ (OA) $x$ ( $10^{-8}$ cm)	$R_B$ (OB) $x$ ( $10^{-8}$ cm)
0.0	600	420	130990.5	241676.1	1.7966	2.0745
0.1	580	410	124875.2	226253.7	1.8184	2.0997
0.2	590	410	124906.1	234855.8	1.8165	2.0975
0.3	600	410	124970.9	243454.3	1.8160	2.0970
0.4	600	420	131191.4	243770.6	1.8142	2.0948
0.5	600	420	131223.6	244263.8	1.8039	2.0830
0.6	600	440	144016.5	244533.0	1.8005	2.0791

 TABLE IV Saturation Magnetization ( $\sigma_s$ ), Magnetron number ( $n_B$ ) Curie Temperature ( $T_C$ ) for  $\text{Cu}_{1+x}\text{Mn}_x\text{Fe}_{2-2x}\text{O}_4$ 

Composition ( $x$ )	$\sigma_s$ (emu/gm)	$n_B$ ( $\mu_B$ )		$T_C$ ( $^\circ\text{K}$ )		
		obs.	cal.	A.C. Susc. ( $^\circ\text{K}$ )	D.C. Resis ( $^\circ\text{K}$ )	Laoria method ( $^\circ\text{K}$ )
$\text{CuFe}_2\text{O}_4$	30.20	1.29	1.29	733	727	740
$\text{Cu}_{1.1}\text{Mn}_{0.1}\text{Fe}_{1.8}\text{O}_4$	28.63	1.23	1.24	715	714	720
$\text{Cu}_{1.2}\text{Mn}_{0.2}\text{Fe}_{1.6}\text{O}_4$	25.90	1.11	1.16	705	701	702
$\text{Cu}_{1.3}\text{Mn}_{0.3}\text{Fe}_{1.4}\text{O}_4$	21.82	0.94	0.96	689	691	688
$\text{Cu}_{1.4}\text{Mn}_{0.4}\text{Fe}_{1.2}\text{O}_4$	19.01	0.82	0.84	670	660	662
$\text{Cu}_{1.5}\text{Mn}_{0.5}\text{FeO}_4$	18.71	0.81	0.80	652	648	655
$\text{Cu}_{1.6}\text{Mn}_{0.6}\text{Fe}_{0.8}\text{O}_4$	16.57	0.72	0.76	620	615	610

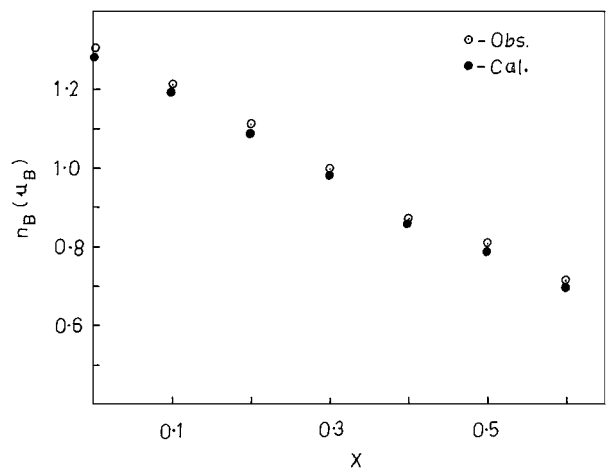
of all the samples have been used to locate the band position and are given in Table III. In the present study the absorption bands of all the ferrites are found to be in the range reported for many other ferrites [26, 27]. The vibrational frequencies depend on the cation mass, cation oxygen distance and bonding force. Waldron [28] and Hafner [29] studied the vibrational spectra of ferrites and attributed high frequency band  $\nu_1$  to the intrinsic vibration of the tetrahedral groups and low frequency band  $\nu_2$  to the intrinsic vibrations of the octahedral group. The high frequency band  $\nu_1$  lies in the range  $600\text{--}580\text{ cm}^{-1}$  and low frequency band  $\nu_2$  lies in the range  $440\text{--}410\text{ cm}^{-1}$ . This difference in band position is expected because of the difference in the  $\text{Fe}^{3+} - \text{O}^{2-}$  distance for the octahedral and tetrahedral co-ordination compounds.

The force constant  $K_t$  (tetrahedral site)  $K_0$  (octahedral sites) have been determined from the IR absorption data using the analysis of Waldron [28]. The bond lengths  $R_A$  and  $R_B$  have been calculated using the formula given by the Gorter [16]. The molecular weights of tetrahedral  $M_t$  and octahedral  $M_o$  sites have been calculated by using cation distribution given in Table II. The values of  $R_A$  and  $R_B$  along with  $K_0$  and  $K_t$  are listed in Table III. It is observed from Table III that the bond stretching for tetrahedral site would lead to higher force constant than that of octahedral site. Our results are in consistent with the results reported by Srivastava *et al.* [30].

The magneton number  $n_B$  was determined from the hysteresis measurements for the respective sample by using the following relation,

$$n_B = \frac{\text{Molecular weight} \times \text{Saturation magnetization}}{5585} \quad (4)$$

The values of saturation magnetization ( $\sigma_s$ ) and magneton number  $n_B$  (saturation magnetization per formula


 Figure 5 Variation of Bohr magneton number ( $n_B$ ) with  $\text{Mn}^{4+}$  content  $x$  for  $\text{Cu}_{1+x}\text{Mn}_x\text{Fe}_{2-2x}\text{O}_4$ .

unit in Bohr magneton) at 300 K for all the samples obtained from magnetization data are listed in Table IV and same are shown in Fig. 5 which shows decrease in  $n_B$  with increase in  $\text{Mn}^{4+}$  content  $x$ . From field dependence of magnetization and observed magnetic moments (Fig. 5 and Table IV) it is clear that the samples with  $x = 0.0$  to  $0.6$  show ferrimagnetic behaviour which decreases with increase in  $x$  values. The observed variation of saturation magnetization with  $\text{Mn}^{4+}$  content can be explained on the basis of cation distribution and Neel's two sub-lattice model.

According to Neel's [31] two sub-lattice model of ferrimagnetism, Neel's magnetic moment per formula unit in  $\mu_B$  is expressed as

$$n_B^N = M_B(x) - M_A(x) \quad (5)$$

where  $M_B$  and  $M_A$  are the B the A sub lattice magnetic moments in  $\mu_B$ . The  $n_B^N$  ( $\mu_B$ ) values for  $\text{Cu}_{1+x}\text{Mn}_x\text{Fe}_{2-2x}\text{O}_4$  were calculated using the cation distribution

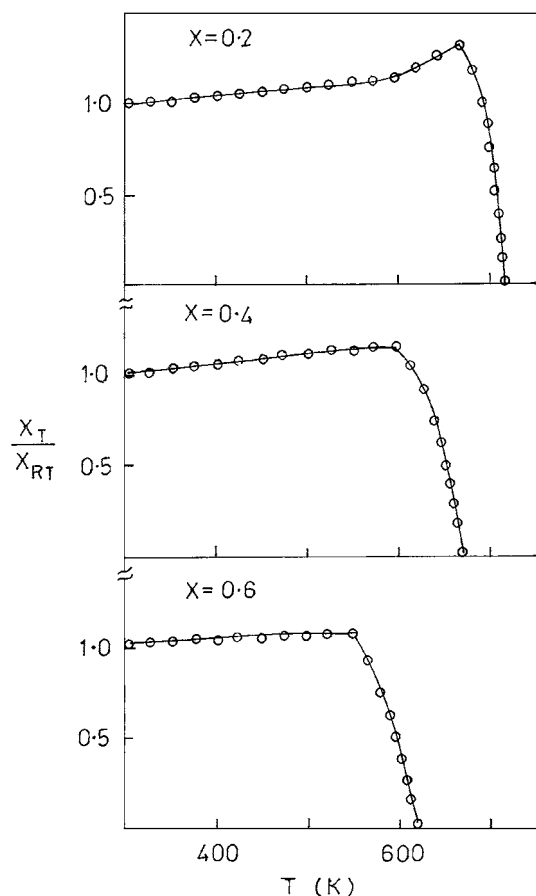


Figure 6 Thermal variation of a.c. susceptibility of  $\text{Cu}_{1+x}\text{Mn}_x\text{Fe}_{2-2x}\text{O}_4$  for  $x = 0.2, 0.4, 0.6$ .

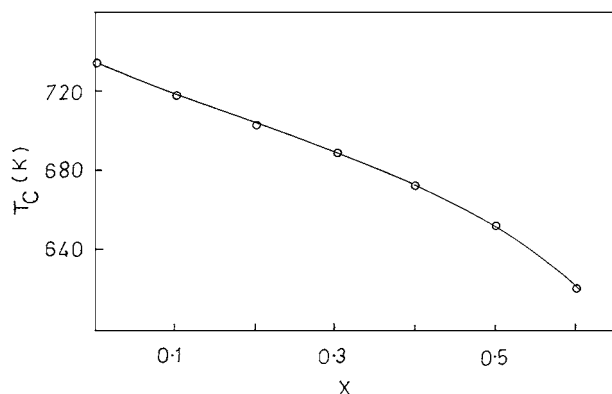


Figure 7 Variation of Curie temperature with  $\text{Mn}^{4+}$  content  $x$  for  $\text{Cu}_{1+x}\text{Mn}_x\text{Fe}_{2-2x}\text{O}_4$ .

(Table II) and ionic magnetic moments of  $\text{Fe}^{3+}$ ,  $\text{Cu}^{2+}$ ,  $\text{Mn}^{4+}$  with their respective values  $5 \mu_B$ ,  $1 \mu_B$  and  $3 \mu_B$ . The calculated values of  $n_B^N$  using the cation distribution (Table II) and Neel's Equation 5, for  $x = 0.0$  to  $0.4$  is valid for the temperature  $0 \text{ K}$ . It is observed from Fig. 5 and Table IV that calculated values are in good agreement with the experimentally found values, confirming collinear spin structure. The cation distribution obtained from magnetization data is very well supported by cation distribution estimated from X-ray intensity ratio calculations.

The typical plots of a.c. susceptibility  $\chi_T/\chi_{RT}$  ( $RT = \text{room temperature}$ ) against temperature  $T$  for the

samples  $x = 0.2, 0.4$  and  $0.6$  are shown in Fig. 6, which exhibit normal ferrimagnetic behaviour. The Curie temperature  $T_C$  determined from the plots ( $\chi_{ac} = 0$ ) are listed in table IV. Fig. 7 depicts the variation of Curie temperature  $T_C$  with  $\text{Mn}^{4+}$  content  $x$  obtained from a.c. susceptibility data. It can be seen from Fig. 7 and Table IV that there is decrease in Curie temperature with the addition  $\text{Mn}^{4+}$  content  $x$ , indicating reduction in ferrimagnetic behaviour. This is attributed to the decreasing A – B interaction resulting from replacement of  $\text{Fe}^{3+}$  ions by  $\text{Mn}^{4+}$  ions on B site and  $\text{Cu}^{2+}$  ions on the A sites. The results of a.c. susceptibility data are in conformity with magnetization results. The Curie temperatures determined from a.c. susceptibility data are in good agreement with those determined from resistivity data and Loaria method (Table IV).

#### 4. Conclusion

From the above experimental results and discussion it can be concluded that X-ray intensity ratio calculation indicate that magnetic  $\text{Mn}^{4+}$  ions occupy octahedral [B] site. Magnetization measurements exhibit Curie's collinear ferrimagnetic structure for  $x = 0.0$  to  $0.6$ , which is very well supported by X-ray intensity calculations. AC susceptibility results suggest normal ferrimagnetic behaviour. The Curie temperature  $T_C$  decreases with increase in  $x$ , is consistent with magnetization data.

#### Acknowledgements

The authors are thankful to Dr. G. K. Bichile, Department of Physics, Dr. Babasaheb Ambedkar Marathwada University, Aurangabad, India for his valuable suggestion and fruitful discussion. The author (D. S. B.) is also thankful to USIC, Shivaji University, Kolhapur for providing X-ray diffractometry charts. The author K. M. Jadhav is thankful to UGC, New Delhi for granting him major research project.

#### References

1. G. BLASSE, *Philips. Res. Rep. Supply* **3** (1964).
2. R. K. DATTA and R. ROY, *J. Amer. Ceram. Soc.* **50** (1967) 578.
3. M. SCHMALZARRIED, *Z. Phys. Chem.* **28** (1961) 108.
4. G. WINKLER, "Magnetic Properties of Materials," edited by J. Smith (Mc Graw-Hill, New York, 1971) p. 22.
5. N. NAMBA and K. KOTHAYASHI, *Jpn. J. Appl. Phys. (Japan)* **17** (1978) 1819.
6. T. YAMASHICO, *ibid.* **12** (1973) 148.
7. S. A. PATIL, S. M. OTARI, V. C. MAHAJAN, M. G. PATIL, A. B. PATIL, M. K. SOUDAGAR, B. L. PATIL and S. R. SAWANT, *Solid St. Commun.* **78** (1991) 39.
8. B. L. PATIL, S. R. SAWANT and S. A. PATIL, *Czech. J. Phys.* **43** (1993) 87.
9. K. P. BELOV, L. G. ANTOSHINA and A. S. MARKOS YAN, *Soviet Phys. Solid St.* **25** (1983) 1609.
10. B. L. PATIL, S. R. SAWANT and S. A. PATIL, *J. Mater. Sci. Lett.* **12** (1993) 399.
11. B. L. PATIL, S. R. SAWANT, S. A. PATIL and R. N. PATIL, *ibid.* **12** (1993) 399.
12. S. A. PATIL, B. L. PATIL, S. R. SAWANT, A. S. JAMBHALE and R. N. PATIL, *Indian J. of Pure and Appl. Phys.* **31** (1993) 904.
13. C. RADHAKRISHANA MURTHY, S. D. LIKHITE and N. P. SHASTRI, *Phil. Mag.* **23** (1971) 503.
14. C. RADHAKRISHANA MURTHY, S. D. LIKHITE and P. W. SAHASTRABUDHE, *Proc. Indian Acad. Sci.* **87A** (1978) 245.

15. S. A. PATIL, B. L. PATIL, S. D. LOTKE and R. N. PATIL, *Phase Transitions* **56** (1996) 29.
16. E. W. GORTER, *Philips. Res. Rep.* **9** (1954) 295.
17. B. D. CULLITY, "Elements of X-ray Diffraction" (Addison-Wesley, Reading, MA, 1959).
18. C. G. WHINFERY, D. W. ECKORT and A. TAUBER, *J. Am. Chem. Soc.* **82** (1960) 2695.
19. S. BHARATI, M. G. GUPTA, A. P. B. SINHA and S. K. DATE, *Indian J. Pure and Appl. Phys.* **18** (1980) 747.
20. S. R. SAWANT and R. N. PATIL, *ibid.* **21** (1983) 145.
21. P. PORTA, F. S. STONE and R. G. TURNER, *J. Solid State Chem.* **II** (1974) 135.
22. M. J. BUEGER, "Crystal Structure Analysis" (John Wiley, New York, 1960).
23. H. FURAHASHI, M. INAGAKI and S. NAKA, *J. Inorg. Nucl. Chem.* **35** (1973) 3003.
24. J. B. GOODENOUGH and A. L. LOEB, *Phys. Rev.* **98** (1953) 391.
25. H. V. KIRAN, A. L. SHASHIMOHAN, D. K. CHAKRABARTY and A. B. BISWAS, *Phys. Stat. Sol. (a)* **66** (1981) 743.
26. S. S. BELLAD, R. B. PUJAR and B. K. CHOUGULE, *Indian J. of Pure and Appl. Phys.* **36** (1998) 598.
27. S. A. PATIL, S. M. OTARI, V. C. MAHAJAN, M. G. PATIL, A. B. PATIL, M. K. SOUDAGAR, B. L. PATIL and S. R. SAWANT, *Solid State Commu.* **78** (1991) 39.
28. R. D. WALDRON, *Phys. Rev.* **99** (1955) 1727.
29. SR. HAFNER, *Z. Krist* **115** (1961) 331.
30. C. M. SRIVASTAVA and T. T. SRINIVASAN, *J. Appl. Phys.* **53** (1982) 8184.
31. L. NEEL, *C. R. Acad. Sci. Paris* **230** (1950) 375.

*Received 11 August 2000  
and accepted 16 October 2001*